Iraqi Journal for Computer Science and Mathematics

Volume 5 | Issue 4 Article 16

2024

The Significance of Cannibalism, Panic, and Sanctuary in the Interactions Between Prey and Predator with a Stage Structure

Ahmed Sami Abdulghafour
Scientific Affairs Department, Al-Iraqia University, Baghdad, Iraq, alania961@gmail.com

Raid Kamel Naji
Department of Mathematics, College of Science, University of Baghdad, Baghdad, Iraq, rknaji@gmail.com

Recommended Citation

Abdulghafour, Ahmed Sami and Naji, Raid Kamel (2024) "The Significance of Cannibalism, Panic, and Sanctuary in the Interactions Between Prey and Predator with a Stage Structure," *Iraqi Journal for Computer Science and Mathematics*: Vol. 5: Iss. 4, Article 16.
DOI: https://doi.org/10.52866/2788-7421.1206
Available at: https://ijcsm.researchcommons.org/ijcsm/vol5/iss4/16

IRAQI JOURNAL FOR COMPUTER SCIENCE AND MATHEMATICS 2024;5:189–207

RESEARCH ARTICLE

The Significance of Cannibalism, Panic, and Sanctuary in the Interactions Between Prey and Predator with a Stage Structure

Ahmed Sami Abdulghafour [a], **Raid Kamel Naji** [b,*]

[a] Scientific Affairs Department, Al-Iraqia University, Baghdad, Iraq
[b] Department of Mathematics, College of Science, University of Baghdad, Baghdad, Iraq

ABSTRACT

This paper analyzes a novel prey-predator model that takes into account the predator's stage structure, cannibalism within the predator population, panicky behavior, and the existence of a sanctuary where the prey might hide from the predator. The Holling type II functional response is used in the predation process. The behavior of the identified fixed points of the proposed system has been closely analyzed. The analysis focuses on the local stability and potential bifurcations that could happen close to the system's fixed points. The Lyapunov function approach is used to investigate the fixed-point stability zone globally. Numerical simulations were run to confirm the analytical findings as well as to test the model's long-term behavior to understand the impact of changing the system's parameters. It is noted that the system exhibits a variety of local bifurcations, most notably the Hopf bifurcation, which is calculated numerically for various parameters.

Keywords: Cannibalism, Panic, Sanctuary, Stage structure, Stability, Bifurcation

1. Introduction

When predators use alternate survival techniques in response to a lack of food resources, the dynamics of prey-predator interactions receive relatively less attention. The majority of research in mathematical ecology focuses on prey species that are directly preyed upon. The Lotka-Volterra model, which Lotka and Volterra first introduced as independent works, is currently used as a framework to clarify the dynamics of prey-predator relationships [1]. Many living things should be classified as either immature or mature in the real world. Between these stages, there may be discernible physical and behavioral differences. For instance, young species lack the ability to reproduce and hunt, and their capacity for survival and defense is minimal. On the other hand, mature organisms have significant survival and defense abilities in addition to reproductive and predatory abilities. These will have a significant effect on the population's dynamic behavior. Studying the prey-predator model with stage structure is, therefore, more useful. As a result, numerous researchers have examined various prey-predator systems with stage structure and provided pertinent dynamic analyses [2–9].

Generally speaking, cannibalism refers to the practice of eating a member of the same species for food. Both marine and land populations exhibit cannibalism, a frequently seen intraspecific interaction [10]. Since individuals often turn to eating other members of their own species to augment their diet, cannibalism is more common in areas with poor nutrition. By reducing possible competition for vital resources such as nourishment,

Received 9 October 2023; accepted 31 July 2024.
Available online 28 November 2024

* Corresponding author.
E-mail addresses: alania961@gmail.com (A. S. Abdulghafour), rknaji@gmail.com (R. K. Naji).

https://doi.org/10.52866/2788-7421.1206

housing, and territoriality, cannibalism acts as a population control mechanism by making those resources easier to come by. Despite the possible benefits it might have for an individual, research has shown that cannibalism is linked to a lower-than-expected survival rate for the group as a whole and a higher risk of eating a family member. Further negative effects, such as a raised risk of disease transmission, are possible as the number of interactions between hosts rises. Contrary to popular assumption, cannibalism does not only occur in extreme cases of food scarcity or unnatural or artificial settings. Numerous species have been found to naturally have it [11]. A particular species' prey [12] and predator [9, 13] can both engage in cannibalism. It may be concluded that there are significant differences between studies focusing on the traditional prey-predator paradigm and those conducted on various prey-predator interactions. According to Deng et al. [14], prey species with a high rate of cannibalism have an advantage in their particular settings. Additionally, they discovered that the main causes of prey extinction are predator species with a higher propensity for cannibalism. According to Zhang et al. (2019), both cannibalism and the economic benefits of cannibalistic behavior have a significant impact on the system's dynamics [15]. As the cannibalism parameter fluctuates towards the coexistence steady state, the stability of the system experiences numerous variations. A noteworthy finding is that the system stabilizes the world even when there is significant cannibalism. To clarify the dynamics between predators and prey, Rayungsari et al. [16] have looked at a mathematical model that incorporates predator cannibalism and refuge. The Lotka-Volterra kind of functional response was used to explain the food transmission phenomenon. Predator cannibalism and refuge are included as variables in the mathematical model created and examined by the authors of past research [13] to fully depict the dynamics of prey-predator interaction. The researchers put out the theory that the prey population demonstrates traits of both refuge reliance on a predator and predation fear.

In addition to cannibalistic behavior, the study of prey-predator interactions is fascinating because of the prey's propensity to hide from capture and ward off predator attacks. From an ecological standpoint, the action that was seen can be categorized as sanctuary-seeking. Our understanding of the complex connection between prey and predator has improved as a result of the development of analytical techniques and computerization. These technological advancements have made it easier to provide more accurate ecological system representations, which has improved understanding of this dynamic relationship. Prey-hiding behavior has been recognized as a key component of prey-predator systems, and the impact of this behavior on system stability has been thoroughly examined in different models [17] and the references therein.

The term "sanctuary" has historically been used to refer to prey that consistently displays some level of resistance to predators. The incorporation of sanctuaries by prey species may have a stabilizing influence on the dynamics of prey-predator interactions, according to some preliminary theoretical analyses. Other models, however, fail to consistently show this straight tendency [18–22]. A few studies [23–26] have used a prey-predator model system where the prey sanctuary is distributed equally between both species. But taking into account the proportionate sanctuary of prey for both species makes our model system seem more realistic. This is because in some natural systems, both the population sizes of predators and prey may have an impact on the availability of prey sanctuary.

The impact of a novel predator that doesn't directly kill prey on prey population sizes has since been the subject of multiple scientific studies [27–35]. "Prey-induced dread" is a term used to describe the phenomenon that is characterized by a decline in the birth rate of prey organisms. Predator presence causes panic in prey species, which makes them avoid open areas and limits their capacity to engage in common behaviors such as mating. Therefore, they have less reproductive potential as a result of their panic due to predators. As a contributing cause of a drop in fertility rates, panic should be considered.

Wang et al.'s prey-predator model [27] examined the impact of panic on prey reproductive dynamics. Additionally, the idea that a higher level of worry can aid in the system's stabilization by completely removing the possibility of occasional alterations was clarified. Panday et al. [28] also looked into how panic affected a Holling type II functional response in a tri-trophic food chain model. It has been deduced that altering panic parameters may be able to control chaotic oscillations based on the finding that the system displays chaotic dynamics for lower levels of both variables. The creation of a prey refuge is a useful tactic for reducing the likelihood of predators overusing the biomass of prey. Panic was covered in various environmental models recently [29–35], and it was mostly observed that fear has a stabilizing effect on the dynamic behavior of the model under study. This paper, however, examines cannibalism, predator-dependent refuge, and fear within the predator population simultaneously, in contrast to the findings indicated above.

Table 1. The description of parameters.

Parameter	Description
r	The birth rate of X in the absence of Z
d_1	The mortality rate of X
b	The intraspecific competition of X
$f \geq 0$	The panic level in X population
a_1	The attack rate of Z to X
K_1	The half-saturation constant
$c \geq 0$	The sanctuary level
μ	Maturity rate
$a_2 = \varepsilon a_1; \varepsilon \in (0, 1)$	The conversion rate of X into Y biomass
a_3	The birth rate due to the cannibalism process
d_2	The mortality rate of Y
e	The cannibalism rate of Z to Y
K_2	The half-saturation constant of Z
$m \in [0, 1]$	The sanctuary rate of Y from the cannibal Z
d_3	The mortality rate of Z

2. Mathematical structure

In this section, the mathematical structure of the interaction between prey and predator, which is divided into juvenile and adult systems, is built. It is suggested that there is cannibalism, panic, and sanctuary within the system. As a result of the ferocity of an adult predator and the resulting panic from that ferocity and aggressiveness, it is assumed that the prey took several safe sanctuaries to protect itself from predation, as the number of safe sanctuaries is proportional to the density of the community of predators attacking it. The predator has the property of internal predation (cannibalism) when there is a lack of food available for it to survive, as previous studies have proven the presence of this property in many animals. Therefore, according to these hypotheses, the dynamics of such an ecological system can be described mathematically utilizing the following set of nonlinear differential equations.

$$\begin{aligned}
\frac{dX}{dT} &= \frac{rX}{1+fZ} - d_1X - bX^2 - \frac{a_1(1-cZ)XZ}{K_1 + X(1-cZ)} = \mathcal{F}_1(X, Y, Z), \\
\frac{dY}{dT} &= \frac{a_2(1-cZ)XZ}{K_1 + X(1-cZ)} + a_3Y - (d_2+\mu)Y - \frac{e(1-m)YZ}{K_2 + (1-m)Y} = \mathcal{F}_2(X, Y, Z) \\
\frac{dZ}{dT} &= \mu Y - d_3Z = \mathcal{F}_3(X, Y, Z), \ ,
\end{aligned} \tag{1}$$

where $X(0) \geq 0$, $Y(0) \geq 0$, and $Z(0) \geq 0$. System (1)'s interaction functions are clearly continuous and have continuous derivatives. Thus, since they are Lipschitzian functions, the system (1) has a unique solution. The parameters of the system are supposed to be nonnegative and have a meaning as given in Table 1.

Theorem 2.1: *The positive cone (int. $\mathbb{R}^3_+$) is positively invariant for the system (1).*

Proof. Use a justification similar to that stated in lemma (2.1) [36]. If you can demonstrate that for all $T \in [0, \tau]$, $X(T) > 0$, $Y(T) > 0$, and $Z(T) > 0$, where τ is any positive real number, then it is enough. Utilizing a contradiction will therefore result in that.

If the situation were reversed, $X(T) > 0$, $Y(T) > 0$, and $Z(T) > 0$ for every $T \in [0, \tau_0]$, respectively, and at least one of $X(\tau_0)$, $Y(\tau_0)$, and $Z(\tau_0)$ must disappear when τ_0 exists with $0 < \tau_0 < \tau$. As a result, system (1) provides

$$\left.\begin{aligned}
X(T) &= X(0)\, e^{\int_0^T \left(\frac{\mathcal{F}_1(X,Y,Z)}{X}\right) dT} \\
Y(T) &= Y(0)\, e^{\int_0^T \left(\frac{\mathcal{F}_2(X,Y,Z)}{Y}\right) dT} \\
Z(T) &= Z(0)\, e^{\int_0^T \left(\frac{\mathcal{F}_3(X,Y,Z)}{Z}\right) dT}
\end{aligned}\right\}$$

Given that $\mathcal{F}_i(X, Y, Z),\ i = 1, 2, 3$ are defined on $[0, \tau_0]$ and are continuous there, $L \geq 0$ exists such that for all $T \in [0, \tau_0]$

$$\left.\begin{aligned} X(T) &= X(0)\, e^{\int_0^T \left(\frac{\mathcal{F}_1(X,Y,Z)}{X}\right) dT} \geq X(0)\exp(-\tau_0 L) \\ Y(T) &= Y(0)\, e^{\int_0^T \left(\frac{\mathcal{F}_2(X,Y,Z)}{Y}\right) dT} \geq Y(0)\exp(-\tau_0 L) \\ Z(T) &= Z(0)\, e^{\int_0^T \left(\frac{\mathcal{F}_3(X,Y,Z)}{Z}\right) dT} \geq Z(0)\exp(-\tau_0 L) \end{aligned}\right\}$$

Hence as $T \to \tau_0$, it gets

$$\left.\begin{aligned} X(\tau_0) &\geq X(0)\exp(-\tau_0 L) \\ Y(\tau_0) &\geq Y(0)\exp(-\tau_0 L) \\ Z(\tau_0) &\geq Z(0)\exp(-\tau_0 L) \end{aligned}\right\}$$

The assumption that at least one of $X(\tau_0)$, $Y(\tau_0)$, and $Z(\tau_0)$ must perish is contradicted by this. Since $X(t) > 0$, $Y(t) > 0$, and $Z(t) > 0$ are all true for every $T \in [0, \tau]$, the proof is complete.

Theorem 2.2: *All system (1) 's solutions are uniformly bounded.*

Proof. From system (1), it is obtained that

$$\frac{dX}{dT} \leq X(r - bX).$$

Therefore, Using lemma (2.2) of [37], it is obtained that $X \leq \frac{r}{b}$ as $T \to \infty$. Define that $N = X + \frac{a_1}{a_2}Y + \frac{a_1}{a_2}Z$, then compute the derivative of N for T to yield

$$\frac{dN}{dT} = X\left(\frac{r}{1+fZ} - d_1 - bX\right) + \frac{a_1}{a_2}Y\left(a_3 - d_2 - \frac{e(1-m)Z}{K_2 + (1-m)Y}\right) - \frac{a_1}{a_2}d_3 Z.$$

Then it is obtained that

$$\frac{dN}{dT} \leq rX - \frac{a_1(d_2 - a_3)}{a_2}Y - \frac{a_1 d_3}{a_2}Z \leq 2\frac{r^2}{b} - \rho N$$

where $\rho = min\{r, d_2 - a_3,\ d_3\}$. Thus, with the help of lemma (2.1) [37], as $T \to \infty$, it is obtained that $N \leq \frac{2r^2}{\rho b}$. Therefore, the proof is complete.

3. Stability and bifurcation

In this section, the local behavior of system (1) around its fixed points (FPs) along with bifurcation are investigated. First, the forms and existence conditions of all possible FPs are determined below.

- The vanishing fixed point (VFP), $n_0 = (0, 0, 0)$, always exists
- The axial fixed point (AFP), $n_1 = (\tilde{X}, 0, 0)$, where $\tilde{X} = \frac{r-d_1}{b}$ exists under the prey survival condition $r - d_1 > 0$.
- The planar fixed point (PFP), $n_2 = (0, \bar{Y}, \bar{Z})$, where

$$\bar{Y} = \frac{(-\mu + a_3 - d_2)d_3 K_2}{(1-m)(e\mu + \mu d_3 - a_3 d_3 + d_2 d_3)}, \bar{Z} = \frac{\mu \bar{Y}}{d_3} \tag{2}$$

exists provided that

$$\mu + d_2 < a_3 < \frac{e\mu}{d_3} + \mu + d_2. \tag{3}$$

• The survival fixed point (SFP), $n_3 = (\hat{X}, \hat{Y}, \hat{Z})$, where

$$\left.\begin{aligned} \hat{X} = \frac{d_3K_1[-\hat{Z}(1-m)(e\mu+(\mu-a_3+d_2)d_3)-(\mu-a_3+d_2)\mu K_2]}{(1-c\hat{Z})[\hat{Z}(1-m)d_3(e\mu-\mu a_2+(\mu-a_3+d_2)d_3)-(\mu a_2-(\mu-a_3+d_2)d_3)\mu K_2]} \\ \hat{Y} = \frac{d_3}{\mu}\hat{Z} \end{aligned}\right\} \tag{4}$$

while $\hat{Z}$ represents a positive root of the below six-order equation.

$$M_6Z^6 + M_5Z^5 + M_4Z^4 + M_3M^3 + M_2M^2 + M_1Z + M_0 = 0, \tag{5}$$

with

$$M_6 = -c^2(1-m)^2 f a_1 d_3^2[(e-a_2)\mu + d_3(\mu-a_3) + d_2d_3]^2 < 0$$

$$M_0 = [\mu a_2(r-d_1) - d_3(\mu-a_3+d_2)(r-d_1+bK_1)]a_2\mu^3K_1K_2^2$$

The formulas for the other coefficients, which were calculated using Mathematica software, are complicated. As a result, if $M_0 > 0$, the equation (5) has at least one positive root. As a consequence, the SFP occurs solely if (5) has a single positive root and the following circumstances are true.

$$\left.\begin{aligned} -\hat{Z}(1-m)\left(e\mu+\left(\mu-a_3+d_2\right)d_3\right)-\left(\mu-a_3+d_2\right)\mu K_2 < 0 \\ \hat{Z}(1-m)\,d_3\left(e\mu-\mu a_2+\left(\mu-a_3+d_2\right)d_3\right)-\left(\mu a_2-\left(\mu-a_3+d_2\right)d_3\right)\mu K_2 < 0 \end{aligned}\right\} \tag{6}$$

Or otherwise,

$$\left.\begin{aligned} -\hat{Z}(1-m)\left(e\mu+\left(\mu-a_3+d_2\right)d_3\right)-\left(\mu-a_3+d_2\right)\mu K_2 > 0 \\ \hat{Z}(1-m)\,d_3\left(e\mu-\mu a_2+\left(\mu-a_3+d_2\right)d_3\right)-\left(\mu a_2-\left(\mu-a_3+d_2\right)d_3\right)\mu K_2 > 0 \end{aligned}\right\} \tag{7}$$

In the following theorems, the local behavior near the above FPs is studied.

Theorem 3.1: *The VFP in system (1) is a stable node (STN) if the following requirements hold*

$$r < d_1 \tag{8}$$

$$a_3 < \mu + d_2 \tag{9}$$

It becomes unstable and the system encounters a transcritical bifurcation (TB) near VFP when $r = d_1 (\equiv r^{TB})$.

Proof. The variational matrix (VM) of system (1) at $n_0 = (0, 0, 0)$ is computed as follows:

$$\mathcal{V}(n_0) = \begin{bmatrix} r-d_1 & 0 & 0 \\ 0 & -\mu+a_3-d_2 & 0 \\ 0 & \mu & -d_3 \end{bmatrix}$$

Hence, $\mathcal{V}(n_0)$ has the eigenvalues $\ell_{10} = r - d_1$, $\ell_{20} = -\mu + a_3 - d_2$, and $\ell_{30} = -d_3$. Consequently, $\ell_{10} < 0$, $\ell_{20} < 0$ under the conditions (8) and (9), respectively, which leads n_0 to become STN. Now when $r = r^{TB}$, then ℓ_{10} becomes zero. So, VFP is a non-hyperbolic point for which there is a possibility of having a bifurcation.

Now, direct computation at $r = r^{TB}$ shows that $\mathcal{U}_0 = (1, 0, 0)^T$ and $\mathcal{W}_0 = (1, 0, 0)^T$ are the eigenvectors related to $\ell_{10} = 0$ for $\mathcal{V}(n_0, r^{TB})$ and $[\mathcal{V}(n_0, r^{TB})]^T$. Also,

$$\mathcal{W}_0{}^T\left[\frac{d\mathcal{F}}{dr}\left(n_0, r^{TB}\right)\right] = 0, \text{ where } \mathcal{F} = (\mathcal{F}_1, \mathcal{F}_2, \mathcal{F}_3)^T$$

$$\mathcal{W}_0{}^T\left[\frac{d}{d\mathcal{X}}\mathcal{F}_r\left(n_0, r^{TB}\right)\mathcal{U}_0\right] = 1 \neq 0$$

where $\mathcal{X} = (X, Y, Z)^T$

$$\mathcal{W}_0{}^T\left[\frac{d^2}{d\mathcal{X}^2}\mathcal{F}\left(n_0, r^{TB}\right).\left(\mathcal{U}_0, \mathcal{U}_0\right)\right] = -2b \neq 0$$

Thus by Sotomayor's theorem [38], the TB occurs.

Theorem 3.2: *The AFP in system (1) is STN if condition (9) with the following requirement holds*

$$\frac{\mu\ a_2\left(r-d_1\right)}{\left(r-d_1+bK_1\right)} < d_3\left(\mu - a_3 + d_2\right) \tag{10}$$

It becomes unstable and the system encounters a TB near AFP when $d_3 = \frac{\mu\ a_2(r-d_1)}{(r-d_1+bK_1)(\mu-a_3+d_2)} (\equiv {d_3}^{TB})$.

Proof. The VM of the system (1) at n_1 is computed as follows:

$$\mathcal{V}\left(n_1\right) = \begin{bmatrix} -(r-d_1) & 0 & -\dfrac{(r-d_1)[fr(r-d_1+bK_1)+a_1]}{b^2(r-d_1+bK_1)} \\ 0 & -\mu + a_3 - d_2 & \dfrac{a_2(r-d_1)}{(r-d_1+bK_1)} \\ 0 & \mu & -d_3 \end{bmatrix}$$

Therefore, the characteristic equation (CE) of $\mathcal{V}(n_1)$ can be written as

$$(-(r-d_1)-\ell_1)(\ell_1^2 + (\mu - a_3 + d_2 + d_3)\ell_1 + d_3(\mu - a_3 + d_2) - \frac{\mu\ a_2(r-d_1)}{(r-d_1+bK_1)}) = 0.$$

Clearly, the first term of CE gives the first negative eigenvalue $\updownarrow_{\infty\infty} = -(r-d_1)$ due to the existence condition of n_1. However, the Routh-Hurwitz criterion ensures that the second term of CE has negative real parts roots, namely ℓ_{21} and ℓ_{31}, when their coefficients are positive, which are satisfied under the conditions (9) and (10). Therefore, n_1 is the STN point.

Now, for $d_3 = {d_3}^{TB}$, the absolute limit of the second term of CE becomes zero, which leads to having zero eigenvalues, say $\ell_{21} = 0$. So, AFP is a nonhyperbolic point.

Now, direct computation at $d_3 = {d_3}^{TB}$ shows that $\mathcal{U}_1 = (\theta_1, \theta_2, 1)^T$ and $\mathcal{W}_1 = (0, \theta_3, 1)^T$ are the eigenvectors related to $\ell_{21} = 0$ for $\mathcal{V}(n_1, {d_3}^{TB})$, and $[\mathcal{V}(n_1, {d_3}^{TB})]^T$, where

$$\theta_1 = -\frac{(r-d_1)[fr(r-d_1+bK_1)+a_1]}{b^2(r-d_1+bK_1)(r-d_1)} < 0,$$

$$\theta_2 = \frac{a_2(r-d_1)}{(r-d_1+bK_1)(\mu-a_3+d_2)} > 0,$$

$$\theta_3 = \frac{\mu}{(\mu-a_3+d_2)} > 0.$$

Also, it is obtained that

$$\mathcal{W}_1{}^T[\frac{d\mathcal{F}}{dd_3}(n_1, {d_3}^{TB})] = 0.$$

$$\mathcal{W}_1{}^T[\frac{d}{d\mathcal{X}}\mathcal{F}_{d_3}(n_1, {d_3}^{TB})\mathcal{U}_1] = -1 \neq 0.$$

$$\mathcal{W}_1{}^T\left[\frac{d^2}{d\mathcal{X}^2}\mathcal{F}\left(n_1, {d_3}^{TB}\right).\left(\mathcal{U}_1, \mathcal{U}_1\right)\right] = -\left[\frac{2a_2K_1b\left[c\left(r-d_1\right)-b\theta_1\right]}{\left(r-d_1+bK_1\right)^2} + \frac{2e\left(1-m\right)\theta_2}{K_2}\right]\theta_3 < 0$$

Thus TB occurs.

Theorem 3.3: *The PFP in system (1) is STN if the following requirements hold*

$$\frac{r}{1+f\bar{Z}} < d_1 + \frac{a_1\left(1-c\bar{Z}\right)\bar{Z}}{K_1}. \tag{11}$$

$$a_3 < \mu + d_2 + \frac{e\left(1-m\right)K_2\bar{Z}}{\left[\left(1-m\right)\bar{Y}+K_2\right]^2}. \tag{12}$$

It becomes unstable and the system encounters a TB near PFP when $d_1 = \frac{r}{1+f\bar{Z}} - \frac{a_1(1-c\bar{Z})\bar{Z}}{K_1} (\equiv {d_1}^{TB})$ if the following condition is satisfied:

$$\frac{2\left[\bar{Z}\left(1-c\bar{Z}\right)^2 a_1 - bK_1^2\right]}{K_1^2} - 2\left[\frac{fr}{\left(1+f\bar{Z}\right)^2} + \frac{a_1\left(1-2c\bar{Z}\right)}{K_1}\right]\theta_5 \neq 0. \tag{13}$$

Otherwise, system (1) encounters a pitchfork bifurcation (PB) near PFP provided that

$$\frac{6f^2r\theta_5^2}{\left(1+f\bar{Z}\right)^3} + \frac{6a_1\left[-\bar{Z}\left(1-c\bar{Z}\right)^3 + \left(1-c\bar{Z}\right)\left(1-3c\bar{Z}\right)K_1\theta_5 + cK_1^2\theta_5^2\right]}{K_1^3} \neq 0. \tag{14}$$

Proof. The VM of system (1) at n_2 is computed as follows:

$$\mathcal{V}\left(n_2\right) = \begin{bmatrix} \frac{r}{1+f\bar{Z}} - d_1 - \frac{a_1\left(1-c\bar{Z}\right)\bar{Z}}{K_1} & 0 & 0 \\ \frac{a_2\left(1-c\bar{Z}\right)\bar{Z}}{K_1} & -\mu + a_3 - d_2 - \frac{e\left(1-m\right)K_2\bar{Z}}{\left[\left(1-m\right)\bar{Y}+K_2\right]^2} & -\frac{e\left(1-m\right)\bar{Y}}{\left(1-m\right)\bar{Y}+K_2} \\ 0 & \mu & -d_3 \end{bmatrix}$$

Therefore, the CE of $\mathcal{V}(n_2)$ can be written as

$$\left(\frac{r}{1+f\bar{Z}} - d_1 - \frac{a_1(1-c\bar{Z})\bar{Z}}{K_1} - \ell_2\right)\left({\ell_2}^2 + (\mu - a_3 + d_2 + \frac{e(1-m)K_2\bar{Z}}{\left[(1-m)\bar{Y}+K_2\right]^2} + d_3)\ell_2\right.$$
$$\left. + d_3\left(\mu - a_3 + d_2 + \frac{e(1-m)K_2\bar{Z}}{\left[(1-m)\bar{Y}+K_2\right]^2}) + \frac{\mu\, e(1-m)\bar{Y}}{(1-m)\bar{Y}+K_2}\right) = 0$$

Clearly, the first term of CE gives the first negative eigenvalue $\ell_{12} = \frac{r}{1+f\bar{Z}} - d_1 - \frac{a_1(1-c\bar{Z})\bar{Z}}{K_1}$ due to condition (11). However, the Routh-Hurwitz criterion ensures that the second term of CE has negative real parts roots, namely ℓ_{22}, and ℓ_{32}, if their coefficients are positive, which are satisfied under conditions (11) and (12). Therefore, n_1 is the STN point.

Now, for $d_1 = {d_1}^{TB}$, ℓ_{12} becomes zero, which means $\ell_{12} = 0$. So, AFP is a non-hyperbolic point.

Now, direct computation at $d_1 = {d_1}^{TB}$ shows that $\mathcal{U}_2 = (1, \theta_4, \theta_5)^T$ and $\mathcal{W}_2 = (1, 0, 0)^T$ are the eigenvectors related to $\updownarrow_{\infty\in} = 0$ for $\mathcal{V}(n_2, {d_1}^{TB})$ and $[\mathcal{V}(n_2, {d_1}^{TB})]^T$, where

$$\theta_4 = \frac{d_3a_2\left(1-c\bar{Z}\right)\bar{Z}}{\left[d_3\left(\mu - a_3 + d_2 + \frac{e(1-m)K_2\bar{Z}}{\left[(1-m)\bar{Y}+K_2\right]^2}\right) + \frac{\mu\, e(1-m)\bar{Y}}{(1-m)\bar{Y}+K_2}\right]K_1} > 0,$$

$$\theta_5 = \frac{\mu a_2(1-c\bar{Z})\bar{Z}}{[d_3(\mu - a_3 + d_2 + \frac{e(1-m)K_2\bar{Z}}{\left[(1-m)\bar{Y}+K_2\right]^2}) + \frac{\mu\, e(1-m)\bar{Y}}{(1-m)\bar{Y}+K_2}]K_1} > 0.$$

Also, it is obtained that

$$\mathcal{W}_2^T\left[\frac{d\mathcal{F}}{dd_1}\left(n_2, {d_1}^{TB}\right)\right] = 0$$

$$\mathcal{W}_2^T\left[\frac{d}{dx}\mathcal{F}_{d_1}\left(n_2, {d_1}^{TB}\right)\mathcal{U}_2\right] = -1 \neq 0$$

$$\mathcal{W}_2^T\left[\frac{d^2}{dx^2}\mathcal{F}\left(n_2, {d_1}^{TB}\right)\cdot(\mathcal{U}_2, \mathcal{U}_2)\right] = \frac{2\left[\bar{Z}(1-c\bar{Z})^2 a_1 - bK_1^2\right]}{K_1^2} - 2\left[\frac{fr}{(1+f\bar{Z})^2} + \frac{a_1(1-2c\bar{Z})}{K_1}\right]\theta_5$$

Therefore, TB arises if condition (13) is satisfied. Consider that condition (13) is now broken. Thus, the result is:

$$\mathcal{W}_2^T\left[\frac{d^3}{dx^3}\mathcal{F}\left(n_2, {d_1}^{TB}\right)\cdot(\mathcal{U}_2, \mathcal{U}_2, \mathcal{U}_2)\right] = \frac{6f^2 r\theta_5^2}{(1+f\bar{Z})^3} + \frac{6a_1\left[-\bar{Z}(1-c\bar{Z})^3 + (1-c\bar{Z})(1-3c\bar{Z})K_1\theta_5 + cK_1^2\theta_5^2\right]}{K_1^3}$$

Hence, PB takes place due to condition (14).

Theorem 3.4: *The SFP in the system (1) is STN if the following requirements hold*

$$\frac{\mathcal{Z}(1-c\hat{Z})^2 a_1}{\left[\hat{X}(1-c\hat{Z}) + K_1\right]^2} < b. \tag{15}$$

$$a_3 < \mu + d_2 + \frac{e(1-m)K_2\hat{Z}}{\left[(1-m)\hat{Y} + K_2\right]^2}. \tag{16}$$

$$\hat{Z} < \frac{1}{2c}. \tag{17}$$

$$\frac{\hat{X}a_2\left[\hat{X}(1-c\hat{Z})^2 + (1-2c\hat{Z})K_1\right]}{\left[\hat{X}(1-c\hat{Z}) + K_1\right]^2} < \frac{e(1-m)\hat{Y}}{(1-m)\hat{Y} + K_2}. \tag{18}$$

$$-q_{11}q_{22}q_{33} - q_{11}q_{23}q_{32} + q_{13}q_{21}q_{32} > 0 \tag{19}$$

It becomes unstable and the system encounters a saddle-node bifurcation (SNB) near PFP when $b = \frac{1}{\hat{X}}\left[\frac{\hat{x}\hat{Z}(1-c\hat{z})^2 a_1}{\left[\hat{X}(1-c\hat{Z})+K_1\right]^2} - \frac{q_{13}q_{21}q_{32}}{(q_{23}q_{32}-q_{22}q_{33})}\right] \equiv \left(b^{SNB}\right)$ if the following condition is satisfied.

$$\alpha_{11}\theta_8 + \alpha_{21}\theta_9 \neq 0 \tag{20}$$

where all the unknown symbols are given below.

Proof. The VM of the system (1) at n_3 is computed by:

$$\mathcal{V}(n_3) = \left[q_{ij}\right]_{3\times 3}$$

where

$$q_{11} = \hat{X}\left(-b + \frac{\hat{Z}(1-c\widehat{Z})^2 a_1}{\left[\hat{X}(1-c\hat{Z}) + K_1\right]^2}\right),$$

$$q_{13} = -\hat{X}\left(\frac{fr}{(1+f\hat{Z})^2} + \frac{a_1\left[\hat{X}(1-c\hat{Z})^2 + (1-2c\hat{Z})K_1\right]}{\left[\hat{X}(1-c\hat{Z}) + K_1\right]^2}\right),$$

$$q_{21} = \frac{\hat{Z}(1-c\hat{Z})a_2 K_1}{\left[\hat{X}(1-c\hat{Z}) + K_1\right]^2} > 0,$$

$$q_{22} = -\mu + a_3 - d_2 - \frac{e(1-m)K_2\hat{Z}}{\left[(1-m)\hat{Y} + K_2\right]^2}$$

$$q_{23} = \frac{\hat{X}a_2\left[\hat{X}(1-c\hat{Z})^2 + (1-2c\hat{Z})K_1\right]}{\left[\hat{X}(1-c\hat{Z}) + K_1\right]^2} - \frac{e(1-m)\hat{Y}}{(1-m)\hat{Y} + K_2}$$

$$q_{32} = \mu > 0, q_{33} = -d_3 < 0, q_{12} = q_{31} = 0$$

Direct computation shows that the CE of $\mathcal{V}(n_3)$ can be represented as

$$\ell_3^3 + \mathcal{P}_1\ell_3^2 + \mathcal{P}_2\ell_3 + \mathcal{P}_3 = 0 \tag{21}$$

where

$$\mathcal{P}_1 = -(q_{11} + q_{22} + q_{33})$$

$$\mathcal{P}_2 = q_{11}q_{22} + q_{11}q_{33} + q_{22}q_{33} - q_{23}q_{32}$$

$$\mathcal{P}_3 = q_{11}q_{23}q_{32} - q_{11}q_{22}q_{33} - q_{13}q_{21}q_{32}$$

with

$$\mathcal{A} = \mathcal{P}_1\mathcal{P}_2 - \mathcal{P}_3 = -q_{11}q_{22}(q_{11} + q_{22}) - (q_{11} + q_{22} + q_{33})(q_{22}q_{33} - q_{23}q_{32}) - q_{11}q_{33}(q_{11} + q_{33}) - q_{11}q_{22}q_{33} - q_{11}q_{23}q_{32} + q_{13}q_{21}q_{32}.$$

Following the Routh-Hurwitz criterion, all roots of the CE given by (20) have negative real parts when $\mathcal{P}_1 > 0, \mathcal{P}_3 > 0$, and $\mathcal{A} > 0$ which are satisfied under the conditions (15)-(19). Thus SFP is an STN.

Now, for the value of $b = b^{SNB}$, it is easy to verify that $\mathcal{P}_3 = 0$. Therefore, SFP becomes non-hyperbolic, which means one of the eigenvalues equals zero (say, $\ell_{13} = 0$), and bifurcation could occur.

Now, direct computation at $b = b^{SNB}$ shows that $\mathcal{U}_3 = (\theta_6, \theta_7, 1)^T$ and $\mathcal{W}_3 = (\theta_8, \theta_9, 1)^T$ are the eigenvector related to $\ell_{13} = 0$ for $\mathcal{V}\left(n_3, b^{SNB}\right)$, and $\left[\mathcal{V}\left(n_3, b^{SNB}\right)\right]^T$, where

$$\theta_6 = -\frac{q_{13}}{q_{11}}, \theta_7 = \frac{q_{21}q_{13} - q_{11}q_{23}}{q_{11}q_{22}}, \theta_8 = \frac{q_{21}q_{32}}{q_{11}q_{22}}, \theta_9 = -\frac{q_{32}}{q_{22}}$$

Also, it is obtained that

$$\mathcal{W}_3^T\left[\frac{d\mathcal{F}}{d\,\mathrm{b}}\left(n_3, b^{SNB}\right)\right] = -\theta_8\hat{X}^2 \neq 0$$

Moreover, straightforward computation gives that

$$\frac{d^2}{dX^2}\mathcal{F}\left(n_3, b^{SNB}\right).(U_3, U_3) = (\alpha_{i1})_{3\times 1}$$

where

$$\alpha_{11} = 2\hat{X}\left[\frac{f^2r}{(1+f\hat{Z})^3} + \frac{ca_1K_1\left(\hat{X}+K_1\right)}{\left(\hat{X}(1-c\hat{Z}) + K_1\right)^3}\right] + 2\left[-\frac{fr}{(1+f\hat{Z})^2} - \frac{a_1K_1\left(\hat{X}(1-c\hat{Z}) + K_1 - 2c\hat{Z}K_1\right)}{\left(\hat{X}(1-c\hat{Z}) + K_1\right)^3}\right]\theta_6 - \frac{2\left(b\hat{X}^3(1-c\hat{z})^3 + (1-c\hat{Z})^2\left(3b\hat{X}^2 - \hat{Z}a_1\right)K_1 + 3b\hat{X}(1-c\hat{Z})K_1^2 + bK_1^3\right)\theta_6^2}{\left(\hat{X}(1-c\hat{Z}) + K_1\right)^3}$$

$$\alpha_{21} = -\frac{2a_2K_1\left[c\hat{X}\left(\hat{X}+K_1\right) - \left(\hat{X}(1-c\hat{Z}) + (1-2c\hat{Z})K_1\right)\theta_6 + \hat{Z}(1-c\hat{Z})^2\theta_6^2\right]}{\left(\hat{X}(1-c\hat{Z}) + K_1\right)^3}$$

$$- \frac{2e(1-m)K_2\theta_7\left[\hat{Y}(1-m)+K_2-(1-m)\hat{Z}\theta_7\right]}{\left((1-m)\hat{Y}+K_2\right)^3}.$$

α_{31} =0.

Thus, by using condition (20), it is obtained that:

$$\mathcal{W}_3^T\left[\frac{d^2}{dx^2}\mathcal{F}\left(n_3, b^{SNB}\right)\cdot\left(\mathcal{U}_3,\mathcal{U}_3\right)\right] = \alpha_{11}\theta_8+\alpha_{21}\theta_9 \neq 0$$

Therefore, SNB arises near PFP.

4. Global stability

The Lyapunov function, as shown in the following theorems, is used in this part to analyze the global stability analysis for the fixed points of the system (1).

Theorem 4.1: *Assume that condition (8) with the following conditions are satisfied, then the VFP is a global asymptotic stable (GAS).*

$$a_3 < d_2. \tag{22}$$

Proof. Consider the following candidate Lyapunov function

$$L_0\left(X,Y,Z\right) = X+\frac{a_1}{a_2}\left(Y+Z\right)$$

Clearly, $L_0:\mathbb{R}_+^3\to\mathbb{R}$ is a C^1 positive definite function on $\{(X,\ Y,\ Z)\in\mathbb{R}_+^3 : X\geq 0, Y\geq 0, Z\geq 0\}$. Direct computation shows that:

$$\begin{aligned}\frac{dL_0}{dT} =& \frac{rX}{1+fZ} - d_1X - bX^2 - \frac{a_1(1-cZ)XZ}{K_1+X(1-cZ)} + \frac{a_1}{a_2}\left(\mu Y - d_3Z\right)\\ &+\frac{a_1}{a_2}\left(\frac{a_2 1-cZ)XZ}{K_1+X(1-cZ)} + a_3Y - (d_2+\mu)Y - \frac{e(1-m)YZ}{K_2+(1-m)Y}\right)\end{aligned}$$

Therefore, it is obtained that

$$\frac{dL_0}{dT} < -\left(d_1-r\right)X - \frac{a_1}{a_2}\left(d_2-a_3\right)Y - \frac{a_1}{a_2}d_3Z$$

Conditions (8) and (22) lead to the $\frac{dL_0}{dT}$ being negative definite. Hence, the VFP is GAS.

Theorem 4.2: *Assume that condition (22) with the following condition are satisfied, then the AFP is a GAS.*

$$rf\bar{X} + \frac{a_1\bar{X}}{K_1} < \frac{a_1}{a_2}d_3. \tag{23}$$

Proof. Consider the following candidate Lyapunov function

$$L_1\left(X,Y,Z\right) = \left(X-\bar{X}-\bar{X}\ln\frac{X}{\bar{X}}\right)+\frac{a_1}{a_2}\left(Y+Z\right)$$

Clearly, $L_1 : \mathbb{R}^3_+ \to \mathbb{R}$ is a C^1 positive definite function on $\{(X,\ Y,\ Z) \in \mathbb{R}^3_+ : X > 0, Y \geq 0, Z \geq 0\}$. Direct computation shows that:

$$\frac{dL_1}{dT} = -\frac{rfXZ}{1+fZ} + \frac{rf\bar{X}Z}{1+fZ} - b\left(X-\bar{X}\right)^2 + \frac{a_1\left(1-cZ\right)\bar{X}Z}{K_1+X\left(1-cZ\right)} - \frac{a_1}{a_2}\left(d_2-a_3\right)Y - \frac{a_1}{a_2}\frac{e\left(1-m\right)YZ}{K_2+\left(1-m\right)Y} - \frac{a_1}{a_2}d_3Z$$

Therefore, it is determined that

$$\frac{dL_1}{dT} < -b\left(X-\bar{X}\right)^2 - \frac{a_1}{a_2}\left(d_2-a_3\right)Y - \left(\frac{a_1}{a_2}d_3 - rf\bar{X} - \frac{a_1\bar{X}}{K_1}\right)Z.$$

Thus, conditions (22) and (23) lead to the $\frac{dL_1}{dT}$ being negative definite. Hence, the AFP is a GAS.

Theorem 4.3: *The PFP is a GAS if condition (8) with the following conditions are met.*

$$a_3 < \frac{e\left(1-m\right)\bar{Z}}{\left(K_2+\left(1-m\right)Y_{Max}\right)\left(K_2+\left(1-m\right)\bar{Y}\right)} + d_2 + \mu. \tag{24}$$

$$\left[\frac{e\left(1-m\right)}{K_2\left(K_2+\left(1-m\right)\bar{Y}\right)} - \mu\right]^2 < 4\frac{1}{Y_{Max}}\left[\frac{e\left(1-m\right)\bar{Z}}{\left(K_2+\left(1-m\right)Y_{Max}\right)\left(K_2+\left(1-m\right)\bar{Y}\right)} - a_3 + \left(d_2+\mu\right)\right]d_3. \tag{25}$$

where Y_{Max} is the upper bound for Y.

Proof. Consider the following candidate Lyapunov function

$$L_2\left(X,Y,Z\right) = X + \frac{a_1}{a_2}\left(Y - \bar{Y} - \bar{Y}\ln\frac{Y}{\bar{Y}}\right) + \frac{a_1}{a_2}\frac{\left(Z-\bar{Z}\right)^2}{2}.$$

Obviously, $L_3 : \mathbb{R}^3_+ \to \mathbb{R}$ is a C^1 positive definite function on $\{(X,\ Y,\ Z) \in \mathbb{R}^3_+ : X \geq 0, Y > 0, Z \geq 0\}$. Direct computation shows that:

$$\begin{aligned}\frac{dL_2}{dT} =& \frac{rX}{1+fZ} - d_1X - bX^2 - \frac{\bar{Y}}{Y}\frac{a_1\left(1-cZ\right)XZ}{K_1+X\left(1-cZ\right)} - \frac{a_1}{a_2}d_3\left(Z-\bar{Z}\right)^2 \\ &- \frac{a_1}{a_2}\left[\frac{e\left(1-m\right)}{\left(K_2+\left(1-m\right)Y\right)\left(K_2+\left(1-m\right)\bar{Y}\right)} - \mu\right]\left(Y-\bar{Y}\right)\left(Z-\bar{Z}\right) \\ &- \frac{a_1}{a_2}\frac{1}{Y}\left[\frac{e\left(1-m\right)\bar{Z}}{\left(K_2+\left(1-m\right)Y\right)\left(K_2+\left(1-m\right)\bar{Y}\right)} - a_3 + \left(d_2+\mu\right)\right]\left(Y-\bar{Y}\right)^2\end{aligned}$$

Therefore, it is result that

$$\begin{aligned}\frac{dL_2}{dT} <& -\left(d_1-r\right)X - \frac{a_1}{a_2}\left[\frac{e\left(1-m\right)}{\left(K_2+\left(1-m\right)Y\right)\left(K_2+\left(1-m\right)\bar{Y}\right)} - \mu\right]\left(Y-\bar{Y}\right)\left(Z-\bar{Z}\right) \\ &- \frac{a_1}{a_2}\frac{1}{Y}\left[\frac{e\left(1-m\right)\bar{Z}}{\left(K_2+\left(1-m\right)Y\right)\left(K_2+\left(1-m\right)\bar{Y}\right)} - a_3 + \left(d_2+\mu\right)\right]\left(Y-\bar{Y}\right)^2 - \frac{a_1}{a_2}d_3\left(Z-\bar{Z}\right)^2\end{aligned}$$

Further, simplifying the result.

$$\frac{dL_2}{dT} < -\left(d_1-r\right)X - \frac{a_1}{a_2}\left[p_{22}\left(Y-\bar{Y}\right)^2 + p_{23}\left(Y-\bar{Y}\right)\left(Z-\bar{Z}\right) + p_{33}\left(Z-\bar{Z}\right)^2\right].$$

Clearly, condition (24) guarantees that $p_{22} > 0$. Hence using the given conditions it is obtained that:

$$\frac{dL_2}{dT} < -(d_1 - r)X - \frac{a_1}{a_2}\left[\sqrt{p_{22}}(Y - \bar{Y}) + \sqrt{p_{33}}(Z - \bar{Z})\right]^2$$

Moreover, $\frac{dL_2}{dT}$ is negative definite due to condition (8). Hence, PFP is a GAS.

Theorem 4.4: *The SFP has a basin of attraction that satisfies the following conditions.*

$$\frac{a_1\hat{Z}(1 - c\hat{Z})}{K_1\left[K_1 + \hat{X}(1 - c\hat{Z})\right]} < b. \tag{26}$$

$$m_{12}{}^2 < m_{11}m_{22}. \tag{27}$$

$$m_{13}{}^2 < m_{11}m_{33}. \tag{28}$$

$$m_{23}{}^2 < m_{22}m_{33}. \tag{29}$$

where all the new symbols are given in the proof.

Proof. Consider the following candidate Lyapunov function

$$L_3(X, Y, Z) = \left(X - \hat{X} - \hat{X}\ln\frac{X}{\hat{X}}\right) + \frac{(Y - \hat{Y})^2}{2} + \frac{(Z - \hat{Z})^2}{2}.$$

Obviously, $L_3 : \mathbb{R}^3_+ \to \mathbb{R}$ is a C^1 positive definite function on $\{(X,\ Y,\ Z) \in \mathbb{R}^3_+ : X > 0, Y > 0, Z > 0\}$. Direct computation shows that:

$$\begin{aligned}
\frac{dL_3}{dT} = &-\left[b - \frac{a_1\hat{Z}(1 - cZ)(1 - c\hat{Z})}{[K_1 + X(1 - cZ)]\left[K_1 + \hat{X}(1 - c\hat{Z})\right]}\right](X - \hat{X})^2 - d_3(Z - \hat{Z})^2 \\
&-\left[\frac{e(1 - m)K_2Z}{[K_2 + (1 - m)Y]\left[K_2 + (1 - m)\hat{Y}\right]} - a_3 + d_2 + \mu\right](Y - \hat{Y})^2 \\
&-\left[\frac{rf}{(1 + fZ)(1 + f\tilde{Z})} + \frac{a_1\left[K_1 + \hat{X}(1 - cZ)\right](1 - c\hat{Z})}{[K_1 + X(1 - cZ)]\left[K_1 + \hat{X}(1 - c\hat{Z})\right]}\right](X - \hat{X})(Z - \tilde{Z}) \\
&+\frac{a_2K_1(1 - cZ)Z}{[K_1 + X(1 - cZ)]\left[K_1 + \hat{X}(1 - c\hat{Z})\right]}(X - \hat{X})(Y - \hat{Y}) \\
&-\left[\frac{e(1 - m)\hat{Y}[K_2 + (1 - m)Y]}{[K_2 + (1 - m)Y][K_2 + (1 - m)\hat{Y}]} - \frac{a_2\hat{X}\left[(K_1 + X)(1 - cZ) - cZ[K_1 + X(1 - cZ)]\right]}{[K_1 + X(1 - cZ)][K_1 + \hat{X}(1 - c\hat{Z})]} - \mu\right](Y - \hat{Y})(Z - \hat{Z})
\end{aligned}$$

Further simplifying the result gives

$$\begin{aligned}
\frac{dL_3}{dT} = &-m_{11}(X - \hat{X})^2 - m_{22}(Y - \hat{Y})^2 - m_{33}(Z - \hat{Z})^2 + m_{12}(X - \hat{X})(Y - \hat{Y}) - m_{13}(X - \hat{X})(Z - \tilde{Z}) \\
&-m_{23}(Y - \hat{Y})(Z - \hat{Z})
\end{aligned}$$

Note that, condition (26) guarantees that $m_{11} > 0$, while condition (9) guarantees that $m_{22} > 0$. Further, the rest of the conditions leads to

$$\begin{aligned}
\frac{dL_3}{dT} < &-\frac{1}{2}\left[\sqrt{m_{11}}(X - \hat{X}) - \sqrt{m_{22}}(Y - \hat{Y})\right]^2 - \frac{1}{2}\left[\sqrt{m_{11}}(X - \hat{X}) + \sqrt{m_{33}}(Z - \hat{Z})\right]^2 \\
&-\frac{1}{2}\left[\sqrt{m_{22}}(Y - \hat{y}) + \sqrt{m_{33}}(z - \hat{z})\right]^2
\end{aligned}$$

Thus, the SFP is a GAS within the region that satisfies the above conditions.

5. Numerical simulation

We will numerically analyze the dynamics of system (1) in this section. The objective is to attain the findings from the aforementioned sections and ascertain how parameters affect the dynamics of system (1). We will use the following default parameter settings to begin numerically solving system (1), and we will gradually change each parameter to see how it affects the system's dynamic behavior and, if necessary, identify any bifurcation points.

$$\begin{aligned} &r = 1,\ d_1 = 0.05,\ f = 1,\ b = 0.1,\ a_1 = 0.75,\ K_1 = 1,\\ &c = 0.2,\ a_2 = 0.5,\ a_3 = 0.1,\ d_2 = 0.15,\ \mu = 0.1,\\ &e = 0.2,\ m = 0.5,\ K_2 = 1,\ d_3 = 0.15. \end{aligned} \tag{30}$$

It is discovered that system (1)'s SFP solution was reached using the set (30) of initial points depicted in Fig. 1, which indicates that the SFP that is given by $n_3 = (2.1,\ 1.55,\ 1.03)$ is a sink.

For the ranges $r \in (0, 0.05)$, $r \in [0.05, 0.15]$, and $r > 0.15$ with the rest of the parameters as in (30), system (1)'s solution approaches n_0, n_1, and n_3, respectively as shown in Fig. 1 for $r = 1$ and Fig. 2 for two different values of r in the other ranges. This confirms the obtained results of Theorem 3.1, where $r = 0.05$ is a TB point near VFP, as well as those of Theorem 3.4 regarding the existence of an STN of the SFP.

On the other hand, system (1)'s solution approaches to n_3 and n_1, where $d_1 \in (0, 0.86)$, $d_1 \in [0.86, 1)$ with the remaining parameters as in (30), respectively as explained in Fig. 1 for d_1 in the first range and Fig. 3 for d_1 in the second range. This confirms the result of Theorem 3.3, where $d_1 = 0.86$ represents a TB point.

Now, by using the set of parameters (30) with different values of f, system (1) is solved numerically, and the obtained trajectories are drawn in Fig. 4. According to Fig. 4, the solutions of system (4) approach the SFP for different values of f with a decrease in the sizes of all species as the value of f increases.

Moreover, for the values of b in the ranges $b \in (0, 0.08]$ and $b \in (0.08, 1]$ with the other values of parameters as in set (30), the solution of system (1) approaches a periodic attractor and SFP, respectively as given in Fig. 5. It was noted that the effect of parameters e, c, and K_1 on the dynamics of system (1) is similar to the effect resulting from the change of parameter b with different range sizes for each parameter. Further, increasing the parameter f or increasing the parameter c when the system approaches a periodic attractor restores stability to system (1), and the solution approaches the SFP again, as shown in Fig. 5. This indicates that system (1) has a Hopf bifurcation in addition to other types of local bifurcations given above.

For the ranges $a_1 \in (0, 0.88]$ and $a_1 > 0.88$ keeping the other parameters as in = set (30), the solution of system (1) goes asymptotically to n_3 and periodic attractor, respectively, as shown in Fig. 6. It was obtained that the effect of parameters m and K_2 on the dynamics of system (1) is similar to the influence obtained from the change of parameter a_1 with different range sizes for each parameter. Further, increasing any of

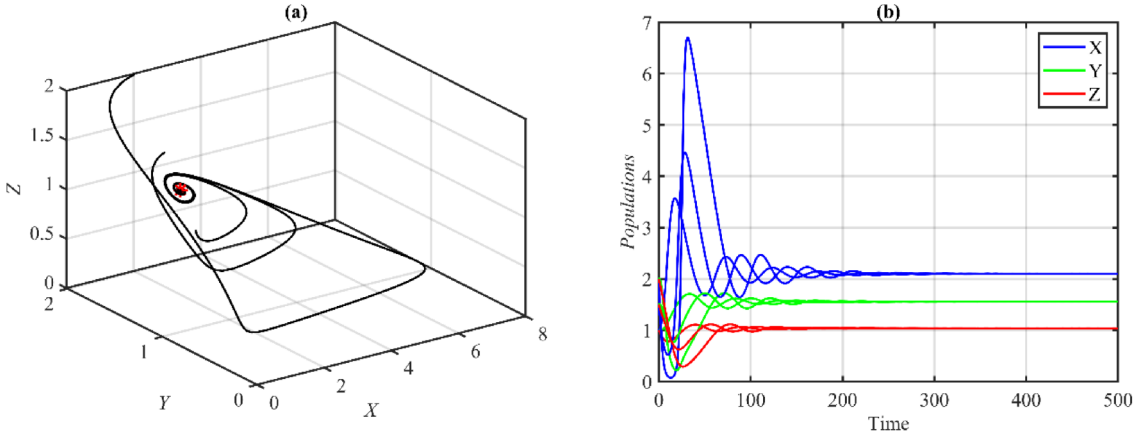

Fig. 1. System (1) approaches SFP using set (30) with different starting points. (a) Phase portrait. (b) Time series of the solution.

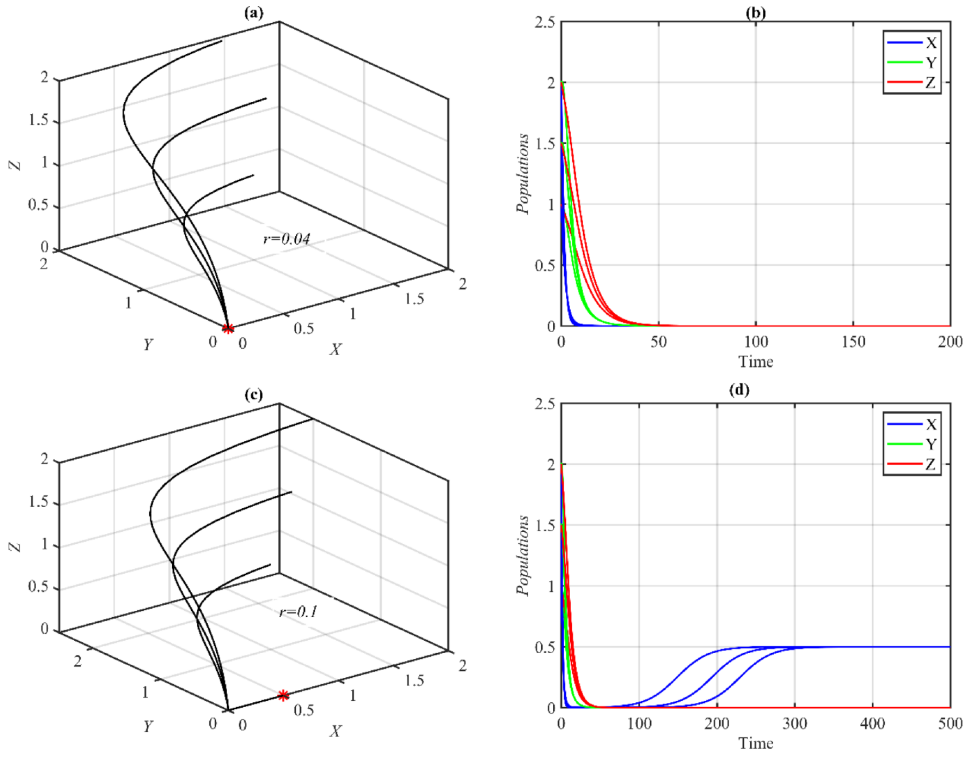

Fig. 2. The solutions of system (1) using set (30) with different starting points. (a) Phase portrait for $r = 0.04$ approaches VFP. (b) Time series of the solution for $r = 0.04$. (c) Phase portrait for $r = 0.1$ approaches AFP, where $n_1 = (0.5, 0, 0)$. (d) Time series of the solution for $r = 0.1$.

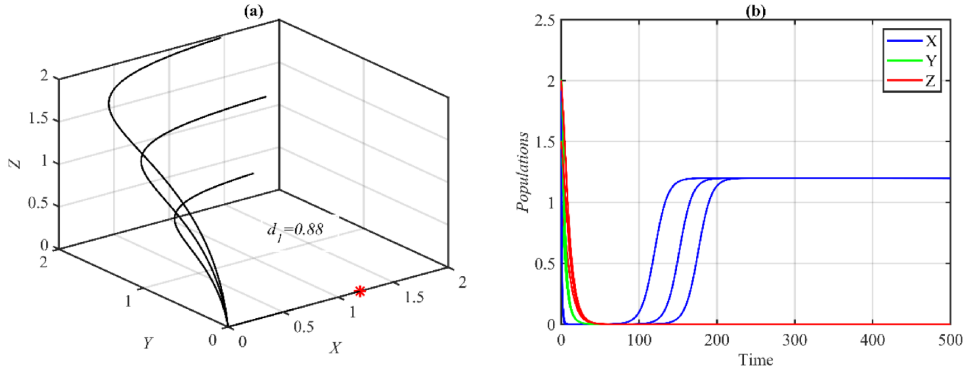

Fig. 3. The solutions of system (1) using set (30) with different starting points. (a) Phase portrait for $d_1 = 0.88$ approaches AFP, where $n_1 = (1.2, 0, 0)$. (b) Time series of the solution for $d_1 = 0.88$.

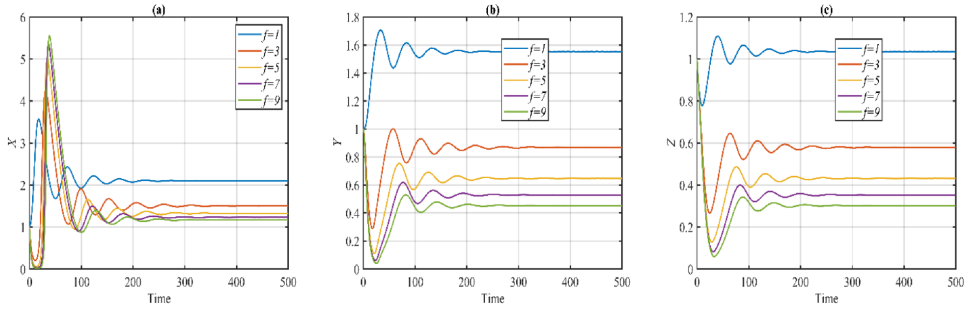

Fig. 4. The solutions of system (1) using set (30) with different values of f. (a) Time series of the trajectories of X. (b) Time series of the trajectories of Y. (c) Time series of the trajectories of Z.

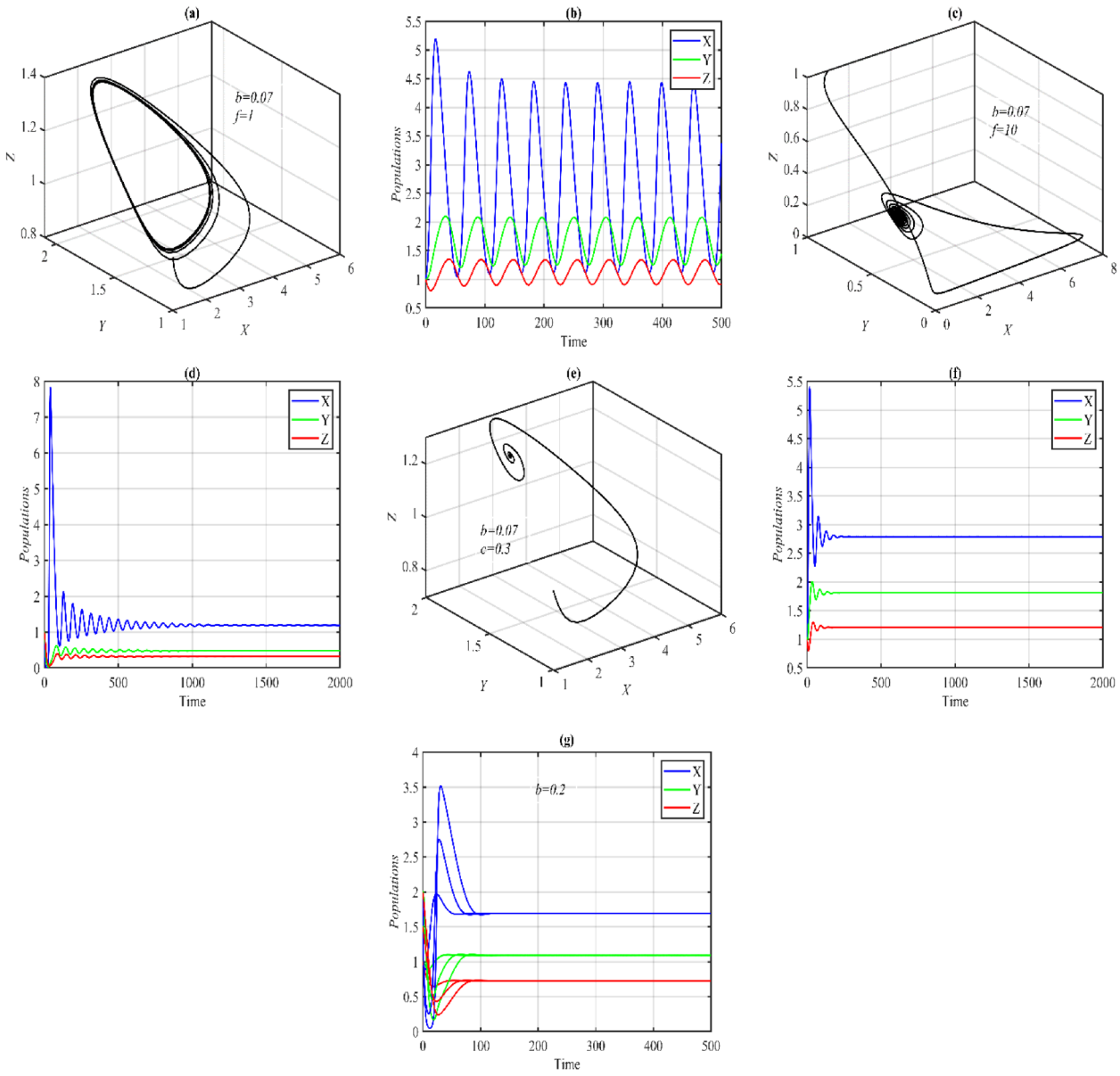

Fig. 5. The solutions of system (1) using set (30). (a) Phase portrait for $b = 0.07$ approaches periodic attractor. (b) Time series of the solution for $b = 0.07$. (c) Phase portrait for $b = 0.07$ with $f = 10$ approaches $n_3 = (1.18, 0.47, 0.31)$. (d) Time series of the solution for $b = 0.07$ with $f = 10$. (e) Phase portrait for $b = 0.07$ with $c = 0.3$ approaches $n_3 = (2.78, 1.81, 1.2)$. (f) Time series of the solution for $b = 0.07$ with $c = 0.3$. (g) Time series of the solution for $b = 0.2$ that approaches $n_3 = (1.69, 1.09, 0.72)$ from different initial points.

the parameters f or c in case of system (1) having a periodic attractor restores stability to the system, and the solution approaches the SFP again, as shown in Fig. 6. This indicates that system (1) undergoes a Hopf bifurcation as a function of parameters a_1, m, and K_2 in addition to other types of local bifurcations discussed in the previous section.

Now, it is observed that the solution of system (1) approaches n_3 periodically and n_2 when $a_3 \in (0, 0.11]$, $a_3 \in (0.11, 0.3)$, and $a_3 \in [0.3, 1]$, respectively with the remaining parameters as in set (30), as shown in Fig. 7. This confirms the results of Theorem 3.3 along with the existence condition of PFP. The existence of a periodic attractor for the first range indicates the occurrence of Hopf bifurcation as a function of the parameter a_3.

Now, for the set of parameters (30) with d_2 in the ranges $d_2 \in (0, 0.14)$, $d_2 \in [0.14, 0.31)$, and $d_2 \in (0.31, 1)$, system (1) approaches asymptotically to the periodic attractor, n_3, and n_1, respectively as shown in Fig. 8. Similar behavior occurs in the case of varying the parameters d_3 regarding the solution of system (1) as shown with d_2.

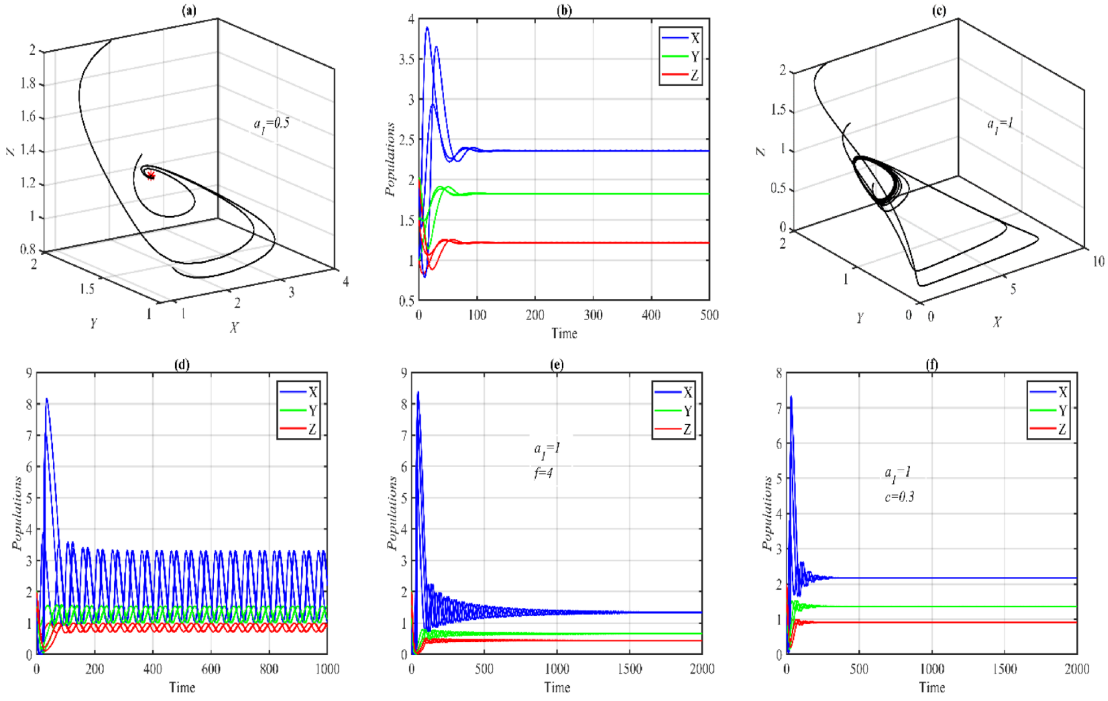

Fig. 6. The solutions of system (1) using set (30) with different initial points. (a) Phase portrait for $a_1 = 0.5$ approaches $n_3 = (2.35, 1.82, 1.21)$. (b) Time series of the solution for $a_1 = 0.5$. (c) Phase portrait for $a_1 = 1$ approaches the same periodic attractor with different phase angles. (d) Time series of the solution for $a_1 = 1$. (e) Time series of the solution for $a_1 = 1$ with $f = 4$ that approaches $n_3 = (1.33, 0.65, 0.43)$. (f) Time series of the solution for $a_1 = 1$ with $c = 0.3$ that approaches $n_3 = (2.17, 1.36, 0.9)$.

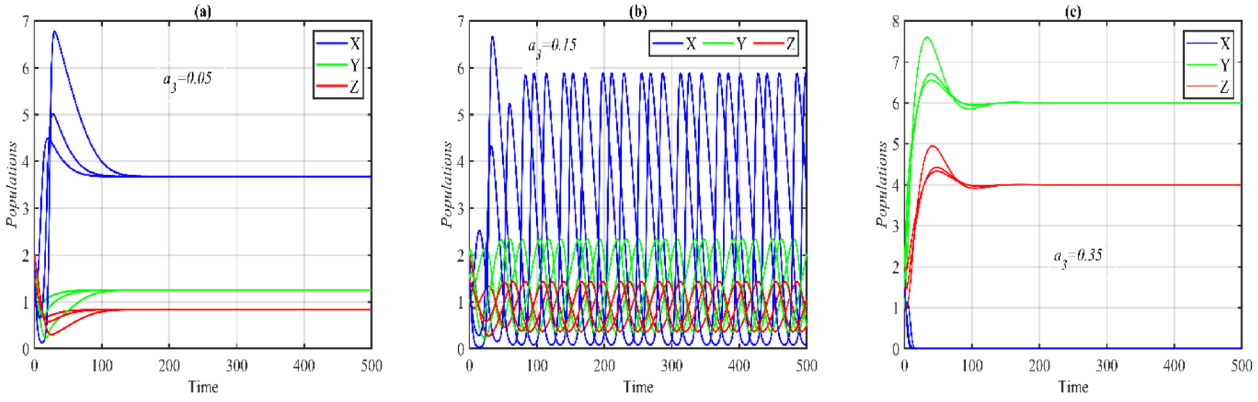

Fig. 7. The solutions of system (1) using set (30) with different initial points. (a) Time series of the solution for $a_3 = 0.05$ that approaches $n_3 = (3.67, 1.24, 0.83)$. (b) Time series of the solution for $a_3 = 0.15$ that approaches a periodic attractor with different phase angles. (c) Time series of the solution for $a_3 = 0.35$ that approaches $n_3 = (0, 6, 4)$.

Finally, for the ranges $\mu \in (0, 0.02]$, $\mu \in (0.02, 0.12)$, and $\mu \geq 0.12$, the solution of system (1) goes to n_1, n_3, and periodic attractor, respectively, as shown in Fig. 9. Similar behavior occurs in the case of varying the parameters a_2 regarding the solution of system (1) as shown with μ.

6. Conclusions

The interaction between prey and predator, which is broken down into juvenile and adult forms, is represented mathematically. It was believed that the predator population would exhibit cannibalism, while the prey population would exhibit panic and sanctuary as defensive traits. A group of nonlinear differential equations were used to model the behavior of such a system. The proposed model's solution's entire qualitative features are investigated. There was a thorough examination of the local stability and bifurcation. The Lyapunov

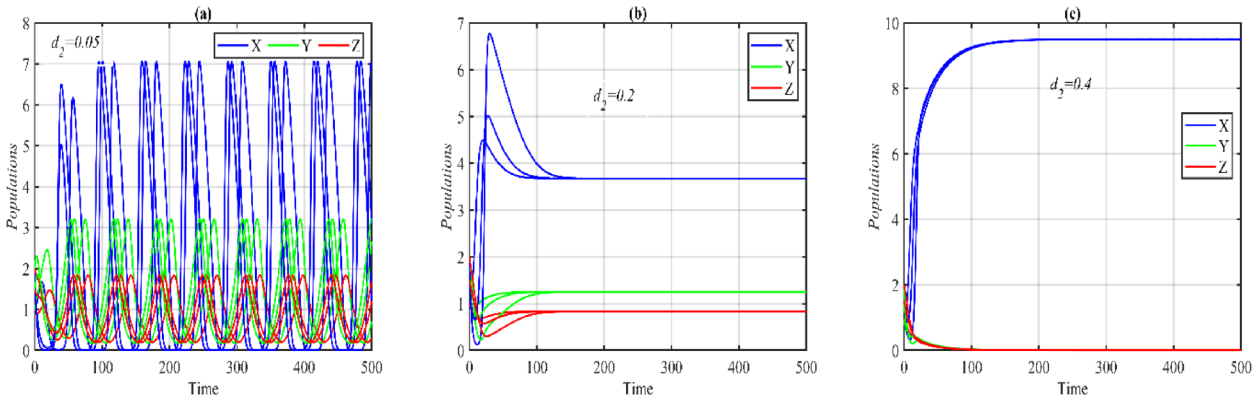

Fig. 8. The solutions of system (1) using set (30) with different initial points. (a) Time series of the solution for $d_2 = 0.05$ that approaches a periodic attractor with different phase angles. (b) Time series of the solution for $d_2 = 0.2$ that approaches $n_3 = (3.67, 1.24, 0.83)$. (c) Time series of the solution for $d_2 = 0.4$ that approaches $n_1 = (9.5, 0, 0)$.

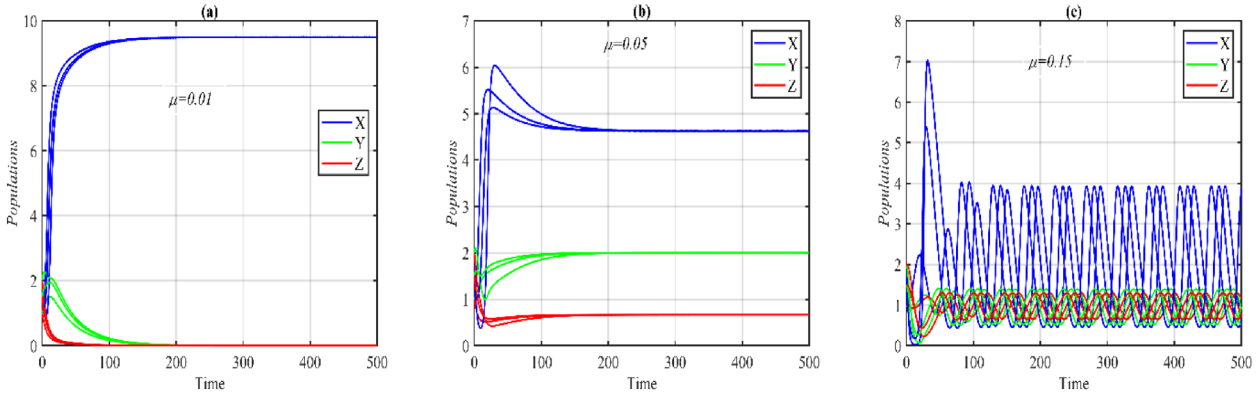

Fig. 9. The solutions of system (1) using set (30) with different initial points. (a) Time series of the solution for $\mu = 0.01$ that approaches $n_1 = (9.5, 0, 0)$. (b) Time series of the solution for $\mu = 0.05$ that approaches $n_3 = (4.62, 2, 0.66)$. (c) Time series of the solution for $\mu = 0.15$ that approaches a periodic attractor with different phase angles.

technique was used to research global stability. The system is solved numerically using the fictitious set of parameters to comprehend how the parameters affect the behavior of the solution to the system. The results are as follows.

The system is dynamically complex and has a wide variety of bifurcations, including Hopf bifurcations. The parameters are separated into four aggregates based on how they affect the solution behavior of the system. The system is stabilized to some extent by the first aggregate, which consists of cannibalistic births and natural deaths in the predator's population (immature and mature) before the system loses its ability to persist. The natural mortality rate of the prey, the rate at which the mature predator attacks the prey, the rate at which the immature predator seeks refuge from the mature predator's cannibals, and the mature predator's half-saturation constant make up the second aggregate, which has the effect of destabilizing the proposed system. The system is stabilized by the third aggregate, which consists of the following parameters: the prey's birth rate, its level of panic, the predator's half-saturation constant, its amount of sanctuary, and its cannibalism rate. Finally, the fourth aggregate, which consists of the rate at which food is transformed from prey to predator and the rate at which the predator reaches maturity, contributes to the system's survival but later destabilizes it.

Acknowledgement

The authors would like to thank the editor and reviewers for their constructive suggestions for improving the presentation of the paper.

Funding

The authors received no specific funding for this work.

Conflicts of interest

The authors declare no conflicts of interest.

References

1. J. D. Murray, “Mathematical biology. I: An Introduction,” 3rd Edition, Springer-Verlag Berlin Heidelberg, 2002.
2. X. A. Zhang, L. S. Chen, and A. U. Neumann, “The stage-structured predator-prey model and optimal harvesting policy,” *Mathematical Biosciences*, vol. 168, no. 2, pp. 201–210, 2000.
3. Y. Lu, K. Pawelek, and S. Liu, “A stage-structured predator-prey model with predation over juvenile prey,” *Applied Mathematics and Computation*, vol. 297, pp. 115–130, 2017.
4. C. Xu, G. Ren, and Y. Yu, “Extinction analysis of stochastic predator-prey system with stage structure and Crowley-Martin functional response,” *Entropy*, vol. 21, no. 3, Article ID 252, 2019.
5. G. P. Neverova, O. L. Zhdanova, B. Ghosh, and E. Frisman, “Dynamics of a discrete-time stage-structured predator-prey system with Holling type II response function,” *Nonlinear Dynamics*, vol. 98, no. 1, pp. 427–446, 2019.
6. B. Ghosh, O. L. Zhdanova, B. Barman, and E. Frisman, “Dynamics of stage-structure predator-prey systems under density-dependent effect and mortality,” *Ecological Complexity*, vol. 41, Article ID 100812, 2020.
7. X. Zhao and Z. Zeng, “Stationary distribution of a stochastic predator-prey system with stage structure for prey,” *Physica A: Statistical Mechanics and its Applications*, vol. 545, Article ID 123318, 2020.
8. Q. Liu, D. Jiang, A. Alsaedi, and B. Ahmad, “Dynamical behavior of a stochastic predator-prey model with stage structure for prey,” *Stochastic Analysis and Applications*, vol. 35, no. 4, pp. 1–21, 2020.
9. H. A. Ibrahim and R. K. Naji, “The complex dynamic in three species food web model involving stage structure and cannibalism”, *AIP Conference Proceedings*, vol. 2292, Article ID 0030510, 2020.
10. V. H. W. Rudolf, “The impact of cannibalism in the prey on predator-prey systems,” *Ecology*, vol. 89, no. 11, pp. 3116–3127, 2008. doi: https://doi.org/10.1890/08-0104.1.
11. K. Takatsu, “Predator cannibalism can shift prey community composition toward dominance by small prey species,” *Ecol. Evol.*, vol. 12, no. 5, p. e8894, 2022. doi: https://doi.org/10.1002/ECE3.8894.
12. A. Basheer, E. Quansah, S. Bhowmick et al., Prey cannibalism alters the dynamics of Holling–Tanner-type predator-prey models. *Nonlinear Dyn.*, vol. 85, no. 4, pp. 2549–2567, 2016.
13. A. S. Abdulghafour and R. K. Naji, “Modeling and analysis of a prey-predator system incorporating fear, predator-dependent refuge, and cannibalism,” *Communications in Mathematical Biology and Neuroscience*, vol. 2022, Article ID 106, 2022. doi: https://doi.org/10.28919/cmbn/7722.
14. H. Deng, F. Chen, Z. Zhu, and Z. Li, “Dynamic behaviors of Lotka–Volterra predator-prey model incorporating predator cannibalism,” *Adv Differ Equ*, vol. 2019, no. 1, Article ID 359, 2019. doi: https://doi.org/10.1186/S13662-019-2289-8/FIGURES/10.
15. F. Zhang, Y. Chen, and J. Li, “Dynamical analysis of a stage-structured predator-prey model with cannibalism,” *Math. Biosci.*, vol. 307, pp. 33–41, 2019. doi: https://doi.org/10.1016/J.MBS.2018.11.004.
16. M. Rayungsari, A. Suryanto, W. M. Kusumawinahyu, and I. Darti, “Dynamical Analysis of a Predator-Prey Model Incorporating Predator Cannibalism and Refuge,” *Axioms*, vol. 11, no. 3, Article ID 116, 2022. doi: https://doi.org/10.3390/AXIOMS11030116.
17. A. S. Abdulghafour and R. K. Naji, “A Study of a Diseased Prey-Predator Model with Refuge in Prey and Harvesting from Predator”. *Journal of Applied Mathematics*, vol. 2018, Article ID 2952791, 2018.
18. Z. Ma, W. Li, Y. Zhao, W. Wang, H. Zhang, and Z. Li, “Effects of prey refuges on a predator-prey model with a class of functional responses: The role of refuges,” *Math Biosci*, vol. 218, no. 2, pp. 73–79, 2009. doi: https://doi.org/10.1016/J.MBS.2008.12.008.
19. B. Sahoo and S. Poria, “Effects of additional food in a delayed predator-prey model,” *Math. Biosci.*, vol. 261, pp. 62–73, 2015. doi: https://doi.org/10.1016/J.MBS.2014.12.002.
20. B. Sahoo, “Dynamical Behaviour of an Epidemic Model with Disease in Top-Predator Population Only: A Bifurcation Study,” *Differential Equations and Dynamical Systems*, vol. 28, no. 1, pp. 153–176, 2016. doi: https://doi.org/10.1007/S12591-016-0307-9.
21. J. Ghosh, B. Sahoo, and S. Poria, “Prey-predator dynamics with prey refuge providing additional food to predator,” *Chaos Solitons Fractals*, vol. 96, pp. 110–119, 2017. doi: https://doi.org/10.1016/J.CHAOS.2017.01.010.
22. S. Khajanchi and S. Banerjee, “Role of constant prey refuge on stage structure predator–prey model with ratio-dependent functional response,” *Appl Math Comput*, vol. 314, pp. 193–198, 2017. doi: https://doi.org/10.1016/J.AMC.2017.07.017.
23. E. González-Olivares, B. González-Yañez, R. Becerra-Klix, and R. Ramos-Jiliberto, “Multiple stable states in a model based on predator-induced defenses,” *Ecological Complexity*, vol. 32, pp. 111–120, 2017. doi: https://doi.org/10.1016/J.ECOCOM.2017.10.004.
24. M. Manarul Haque and S. Sarwardi, “Dynamics of a Harvested Prey–Predator Model with Prey Refuge Dependent on Both Species,” *International Journal of Bifurcation and Chaos*, vol. 28, no. 12, Article ID 1830040, 2018. doi: https://doi.org/10.1142/S0218127418300409.
25. E. A. H. Jabr and D. K. Bahlool, “The Dynamics of a Food Web System: Role of a Prey Refuge Depending on Both Species,” *Iraqi Journal of Science*, vol. 62, no. 2, pp: 639–657, 2021. doi: https://doi.org/10.24996/ijs.2021.62.2.29.

26. H. A. Ibrahim, D. K. Bahlool, H. A. Satar, and R. K. Naji, “Stability and bifurcation of a prey-predator system incorporating fear and refuge”, *Communications in Mathematical Biology and Neuroscience*, vol. 2022, Article ID 32, 2022.
27. X. Wang, L. Zanette, and X. Zou, “Modelling the fear effect in predator-prey interactions,” *J. Math. Biol.*, vol. 73, no. 5, pp. 1179–1204, 2016. doi: https://doi.org/10.1007/S00285-016-0989-1.
28. P. Panday, N. Pal, S. Samanta, and J. Chattopadhyay, “Stability and Bifurcation Analysis of a Three-Species Food Chain Model with Fear,” *International Journal of Bifurcation and Chaos*, vol. 28, no. 1, Article ID 1850009, 2018. doi: https://doi.org/10.1142/S0218127418500098.
29. N. H. Fakhry and R. K. Naji, “The dynamics of a square root prey-predator model with fear”, *Iraqi Journal of Science*, 2020, vol 61, no.1, pp. 139–146, 2020.
30. F. H. Maghool and R. K. Naji, “The Dynamics of a Tritrophic Leslie-Gower Food-Web System with the Effect of Fear”, *Journal of Applied Mathematics*, vol. 2021, Article ID 2112814, 2021.
31. S. Al-Momen and R. K. Naji, “The Dynamics of Modified Leslie-Gower Predator-Prey Model Under the Influence of Nonlinear Harvesting and Fear Effect”, *Iraqi Journal of Science*, vol. 63, no. 1, pp. 259–282, 2022.
32. S. Nadim, S. Samanta, N. Pal, I. M. ELmojtaba, I. Mukhopadhyay, and J. Chattopadhyay, “Impact of Predator Signals on the Stability of a Predator–Prey System: A Z-Control Approach,” *Differ. Equ. Dyn. Syst.*, vol. 30, no. 2, pp. 451–467, 2022. doi: https://doi.org/10.1007/S12591-018-0430-X.
33. N. H. Fakhry, R. K. Naji, S. R. Smith, and M. Haque, “Prey fear of a specialist predator in a tri-trophic food web can eliminate the super predator,” *Front. Appl. Math. Stat.*, vol. 8, 2022. doi: https://doi.org/10.3389/FAMS.2022.963991.
34. A. R. M. Jamil and R. K. Naji, “Modeling and Analysis of the Influence of Fear on the Harvested Modified Leslie–Gower Model Involving Nonlinear Prey Refuge,” *Mathematics*, vol. 10, no. 16, pp. 1–22, 2022. doi: https://doi.org/10.3390/math10162857.
35. Z. S. Abbas and R. K. Naji, “Modeling and Analysis of the Influence of Fear on a Harvested Food Web System,” *Mathematics*, vol. 10, no. 18, 2022. doi: https://doi.org/10.3390/MATH10183300.
36. A. H. Alridha, A. S. Al-Jilawi, and F. H. Abd Alsharify, “Review of Mathematical Modelling Techniques with Applications in Biosciences,” *Iraqi Journal for Computer Science and Mathematics*, vol. 3, no. 1, p. 135–144, 2022. doi: https://doi.org/10.52866/ijcsm.2022.01.01.015.
37. Z.-A. S. A. Rahman, B. H. Jasim, and Y. I. A. Al-Yasiri, “Chaotic Dynamics in the 2D System of Nonsmooth Ordinary Differential Equations,” *Iraqi Journal for Computer Science and Mathematics*, vol. 3, no. 2, p. 8–17, 2022. doi: https://doi.org/10.52866/ijcsm.2022.02.01.002.
38. J. P. Tripathi, S. Abbas, and M. Thakur, “A density-dependent delayed predator-prey model with Beddington-DeAngelis type Function Response incorporating a prey refuge”, *Commun. Nonlin. Sci. Numer. Simulat.* vol 22, pp. 427–450, 2015.
39. F. Chen, “On a nonlinear nonautonomous predator-prey model with diffusion and distributed delay”, *J. Comput. Appl. Math.* vol. 180, pp. 33–49, 2015. doi: https://doi.org/10.1016/j.cam.2004.10.001.
40. Perko, “Differential equations and dynamical systems”, Springer, New York, 3rd edition, 2001